Biological and Medical Applications of Materials and Interfaces

Bioinspired DNA-Inorganic Hybrid Nanoflowers Combined with a Personal Glucose Meter for On-Site Detection of MiRNA

Tingting Wu, Yuemeng Yang, Yu Cao, Yongchao Song, Li-Ping Xu, Xueji Zhang, and Shutao Wang

ACS Appl. Mater. Interfaces, **Just Accepted Manuscript** • DOI: 10.1021/acsami.8b15917 • Publication Date (Web): 20 Nov 2018

Bioinspired DNA-Inorganic Hybrid Nanoflowers Combined with a Personal Glucose Meter for On-Site Detection of MiRNA

Tingting Wu, † *Yuemeng Yang,* † *Yu Cao,* † *Yongchao Song,* † *Li-Ping Xu,**,† *Xueji Zhang,**,† *Shutao Wang*‡

† Research Center for Bioengineering and Sensing Technology, Beijing Key Laboratory for Bioengineering and Sensing Technology, School of Chemistry and Biological Engineering, University of Science and Technology Beijing, Beijing 100083, P. R. China.

‡ CAS Key Laboratory of Bio-inspired Materials and Interfacial Science, CAS Center for Excellence in Nanoscience, Technical Institute of Physics and Chemistry, Chinese Academy of Sciences, Beijing 100190, P. R. China

KEYWORDS : miRNA detection; DNA-inorganic hybrid nanoflower; personal glucose meter; cotton thread

ABSTRACT

Biomineralization is an important process in nature, by which living organisms participate in producing organic/inorganic hybrid materials and the resultant materials showed sophisticated structures and excellent physical and chemical properties. Inspired by biomineralization, DNA-$Cu_3(PO_4)_2$ hybrid nanoflowers (HNFs) were prepared and exhibited high stability, high surface-to-volume ratio, good DNA encapsulation ability. A facile thread platform for miRNA detection was fabricated by employing DNA-$Cu_3(PO_4)_2$ HNFs as captors, and the signal could be easily read out by a personal glucose meter (PGM). The fabricated biosensor could detect miRNA-21 quantitatively and a detection limit of 0.41 nM was achieved. Furthermore, miRNA in A549 cell lysate could also be detected without pretreatment. Based on the bioinspired DNA-inorganic HNFs, this work achieves a fast, simple, low-cost method for specific and sensitive detection of miRNA both in aqueous solution and biological sample, indicating its great promise in biomedical and clinical applications.

INTRODUCTION

In nature, living organisms could participate in producing organic/inorganic hybrid materials, which is an important process called biomineralization. Most biominerals have elaborate hierarchical structures, high mechanical hardness and flexibility, which are not expected in many conventional synthetic materials. Moreover, biomineralization happens under mild conditions at a near-neutral pH and ambient temperature[1-4]. Owing to these fascinating features, biomineralization have attracted

much attention and inspired the fabrication of organic/inorganic hybrid materials. Inspired by biomineralization, several protein-inorganic hybrid nanoflowers (HNFs) have been prepared by mixing protein with a metal ion solution without harmful reagents and extreme operating conditions, and those HNFs exhibited high stability and large surface-to-volume ratio[5-8]. The proteins and enzymes can be immobilized in those HNFs with enhanced activity, stability and selectivity. The protein-inorganic HNFs have been taken as nanobiocatalyst, enzyme reactors, and have many applications in proteomic analysis, biodetection, and the adsorption of toxic heavy metals[9-12]. In addition, some DNA nanoflowers also have been reported in recent years[13-15], which trigged us to broad the concept of protein-inorganic HNFs into nucleic acid-inorganic HNFs, and might bring the new insight for the sensitive miRNA detection.

MicroRNAs (miRNAs) are short, noncoding single-strand RNAs, the aberrant expressions and dysregulation of miRNAs are highly associated with kinds of diseases, especially cancers[16-20]. The traditional miRNA detection methods need time-consuming sample pretreatment, complicated experimental process and high experimental cost, which has dramatically restricted their practical applications on on-site diagnostic testing at low-resource settings[21-24]. Thus the on-site detection for miRNAs are highly desired. Lateral flow nucleic acid biosensors have become the popular on-site diagnostic tools[25-27]. However, only qualitative or semi-quantitative detections can be achieved by comparing the color intensity on the test zone. Personal glucose meter (PGM) is a widely used quantitative device for glucose screening due to its low cost, portable pocket size, simple operation, and reliability[28-30]. Recently, PGMs have been

extended their application for same non-glucose targets screening, such as metal ions, small molecules and proteins[31-35], which offers a new way for on-site diagnostics.

In this work, inspired by biomineralization, DNA-$Cu_3(PO_4)_2$ HNFs were prepared. The as-prepared DNA-$Cu_3(PO_4)_2$ HNFs were used as captors to bind the DNA-invertase conjugates (signal probe) in the presence of miRNA-21. Then a cotton thread was used as a microfluidic channel to separate the HNFs and unbounded DNA-invertase conjugates without tedious washing steps. The unbounded DNA-invertase conjugates were transported to the absorption pad, in which the invertase in conjugates could hydrolyze sucrose into glucose and the target concentration can be quantified according to the signal readout of PGM. Based on the bioinspired DNA-inorganic HNFs, a promising strategy for on-site miRNA detection was provided, which might have potential applications in practical diagnostics.

EXPERIMENTAL SECTION

Materials and reagents. The cotton thread was taken from a store (Beijing, China) and the diameter was 430 ± 17 μm. The absorption pad (H-1), glass fibers (GF-08) were bought from Jiening Biological Technology Co., Ltd. (Shanghai, China). Invertase, sulfosuccinimidyl-4-(N-maleimidomethyl)-cyclohexane-2-carboxylate (sulfo-SMCC), tris(2-carboxyethyl)phosphine (TCEP), sucrose, streptavidin (SA), $CuSO_4{\cdot}5H_2O$ were obtained from Sigma-Aldrich.

Target-miRNA and interference miRNAs were taken from Suzhou Gene-Pharma Co.Ltd. (Suzhou, China).

Target miRNA-21: 5'-UAG CUU AUC AGA CUG AUG UUG A-3'

Interference miRNA-375: 5'-UUU GUU CGU UCG GCU CGC GUG A-3'

Interference miRNA-141: 5'-UAA CAC UGU CUG GUA AAG AUG G-3'

Interference miRNA-1290: 5'-UGG AUU UUU GGA UCA GGG A-3'

The oligonucleotides were obtained from Sangon Biological Engineering Technology & Co. Ltd (Shanghai, China). The oligonucleotide sequences were as follows:

Biotin-DNA1: 5'-TCT GAT AAG CAA AAA AAA AAA/biotin-3'

Thio-DNA2: 5'-thio/AAA AAA AAA ATC AAC ATC AG-3'

Biotin-DNA-cy3: 5'-cy3/TCT GAT AAG CAA AAA AAA AAA/biotin-3'

Instruments. The glucose concentrations were measured by a personal glucose meter obtained from Johnson (OneTouch® SelectSimple, Beijing, China). Cotton threads were treated by vacuum plasma reactor (PDG-MG). A JSM-6700F scanning electron microscope (SEM) (JEOL, Japan) and a FEIF20 transmission electron microscope (TEM) (FEI, USA) were used to characterize the morphologies of the SA-$Cu_3(PO_4)_2$ HNFs. X-ray diffraction (XRD) pattern was recorded by a Bruker-AXS X-ray diffractometer with Cu Kα radiation (λ=1.5418 Å). Fourier transform infrared (FT-IR) spectra were acquired on Nicolet 400 Fouriertransform infrared spectrometer (Madison,WI). X-ray photoelectron spectroscopy (XPS) analysis were examined by an AXIS ULTRA^{DLD} spectrometer (Kratos, Japan).

Preparation of DNA-$Cu_3(PO_4)_2$ HNFs. DNA-$Cu_3(PO_4)_2$ HNFs were synthesized *via* two different approaches. In method 1, the SA-$Cu_3(PO_4)_2$ HNFs were synthesized firstly[6, 8-9]. In brief, SA (20 μL, 5 mg/mL) and $CuSO_4$ solution (6.7 μL, 120 mM) were

added to PBS buffer (1 mL, 30 mM, PH=7.4). After reaction at room temperature for 72 h, the solution was centrifuged (10000 rpm, 10 min), and the SA-$Cu_3(PO_4)_2$ HNFs precipitate was collected and washed for another two times. Then biotin-DNA1 was added into 100 μL 1 mg/mL SA-$Cu_3(PO_4)_2$ HNFs in PBS to form the DNA-$Cu_3(PO_4)_2$ HNFs and reacted for 2 h. Then the precipitate of DNA-$Cu_3(PO_4)_2$ HNFs was collected by centrifugation and washed for another two times with PBS. Finally, the as-obtained precipitate was dispersed in 100 μL PBS. In method 2, biotin-DNA1 was firstly incubated with 20 μL of 5 mg/mL SA for 2 h. Then the mixture and 6.7 μL of 120 mM $CuSO_4$ solution were added to 1 mL PBS buffer (30 mM, PH=7.4). After reaction at room temperature for 72 h, the precipitate of DNA-$Cu_3(PO_4)_2$ HNFs was washed and stored for further use.

For the purpose to prepare the BSA-$Cu_3(PO_4)_2$ HNFs, BSA (20 μL, 5 mg/mL) and $CuSO_4$ solution (6.7 μL, 120 mM) were added to PBS (1 mL, 30 mM, PH=7.4) and reacted for 72 h at room temperature. Then the precipitate of DNA-$Cu_3(PO_4)_2$ HNFs was washed and stored for further use.

Preparation of DNA2-invertase conjugates. The DNA2-invertase conjugates was synthesized according to the previous reports with some modifications[36-37]. Briefly, thio-DNA2 (30 μL, 100 μM), TCEP (2 μL,30 mM) and sodium phosphate buffer (2 μL, 1M, PH = 5.5) were firstly mixed and reacted for 1 h. Subsequently, the thio-DNA2 was purified by Amicon-3K for 8 times using buffer A (0.1 M NaCl, 0.1 M sodium phosphate buffer, PH = 7.3) to remove the excess TCEP. In the meantime, invertase (40 μL, 20 mg/mL) was vortexed with sulfo-SMCC (0.2 mg) in buffer A, and the

soultion was shook for 1h. Then the invertase was firstly centrifuged to remove the insoluble sulfo-SMCC and then purified by Amicon-50K for 8 times using buffer A. Then the activated thio-DNA2 and invertase were mixed and reacted for 48 h. Finally, the mixture was purified by Amicon-50K for 8 times using buffer A and the final volume was 30 μL.

Fabrication of cotton thread-based device. Firstly**,** the vacuum plasma reactor (450 m Torr, 150 mW) was used to treat cotton threads for 5 min. The sample pad (glass fibers, 8 mm × 8 mm) was soaked in a solution (0.15 M NaCl, 0.05 M Tris-HCl and 0.23% Triton X-100) for 1 h, then dried at room temperature for further use. The absorption pad (5 mm × 5 mm) for sucrose immobilization was firstly soaked in 1 M sucrose for 2 h and dried at room temperature. All these three parts were assembled to a plastic pad by double faced adhesive tapes, the cotton thread about 6 cm was hang in the air, the sample pad was at the head end and the absorption pad was at the other end.

Target miRNA-21 detection. 50 μL sample solution in running buffer (PBS) was firstly mixed with DNA-$Cu_3(PO_4)_2$ HNFs and DNA2-invertase conjugates. After being incubated for 1 h, the mixture was added to the sample pad. During the assay process, the solution migrated to the absorption pad (sucrose pad). And 40 μL running buffer was added every 20 min to drive all the unbounded DNA2-invertase conjugates into the sucrose pad and kept the humidity of the sucrose pad as well. For quantitative measurements, a PGM was used to detect the glucose concentration of the solution

which was squeezed out from the sucrose pad. The change of PGM signal before and after the miRNA detection (Δ PGM signal) was used to quantify miRNA-21.

In order to detect target miRNA-21in A549 cell lysate, the mixture of 10 μL cell lysate and 40 μL running buffer was used as the sample solution, and the detection process was followed the procedures described above.

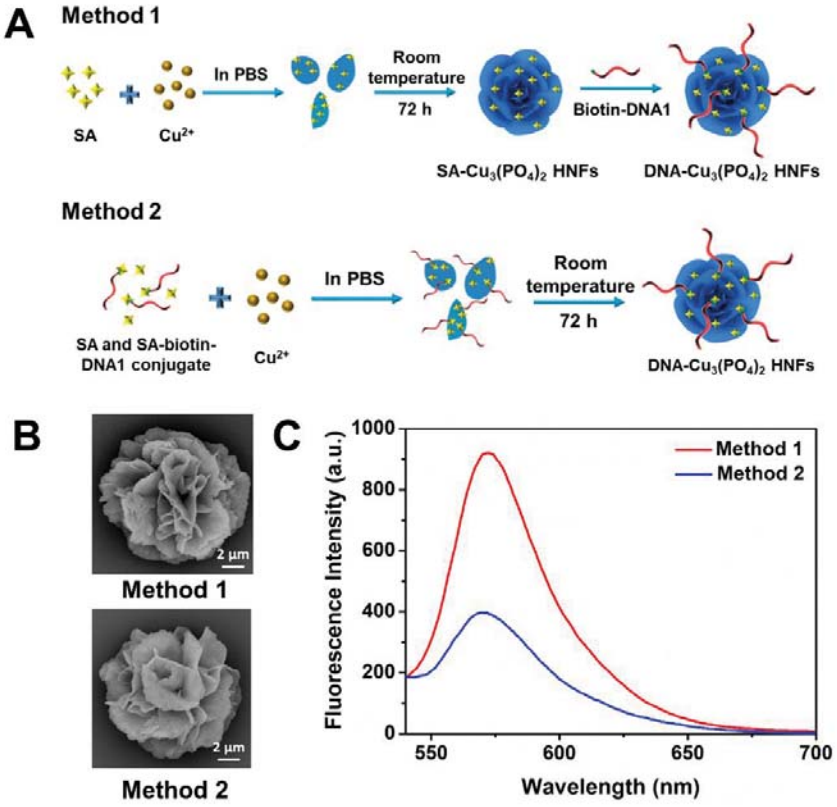

Figure 1. (A) Schematic illustration of two methods for the fabrication of DNA-$Cu_3(PO_4)_2$ HNFs. (B) SEM images of DNA-$Cu_3(PO_4)_2$ HNFs prepared by these two methods. (C) The fluorescence spectra of the DNA-$Cu_3(PO_4)_2$ HNFs synthesized by these two methods after incubation with biotin-DNA-cy3.

RESULTS AND DISCUSSION

Preparation and characterizations of DNA-$Cu_3(PO_4)_2$ HNFs. The DNA-$Cu_3(PO_4)_2$ HNFs were synthesized *via* two methods as illustrated in Figure 1A. In method 1, $CuSO_4$ and SA was mixed with PBS solution and reacted for 72 h to prepare the SA-$Cu_3(PO_4)_2$ HNFs. Then biotin-DNA1 was added and the DNA-$Cu_3(PO_4)_2$ HNFs was formed due to the specific interaction between biotin and SA. In method 2, SA was firstly incubated with the biotin-DNA1, and then mixed with the PBS solution containing Cu^{2+}, the DNA-$Cu_3(PO_4)_2$ HNFs were formed after 72 h. The SEM images in Figure 1B indicated the successful preparation of the DNA-$Cu_3(PO_4)_2$ HNFs by these two different methods and a branched flower-like structure could be observed. In order to compare the DNA encapsulation ability of DNA-$Cu_3(PO_4)_2$ HNFs, cy3 labelled biotin-DNA (biotin-DNA-cy3) was used in the preparation of HNFs. As indicated in Figure 1C, the DNA-$Cu_3(PO_4)_2$ HNFs prepared by method 1 exhibited stronger fluorescence intensity than those prepared by method 2, indicating better DNA encapsulation ability of DNA-$Cu_3(PO_4)_2$ HNFs prepared by method 1, which was used in the following study.

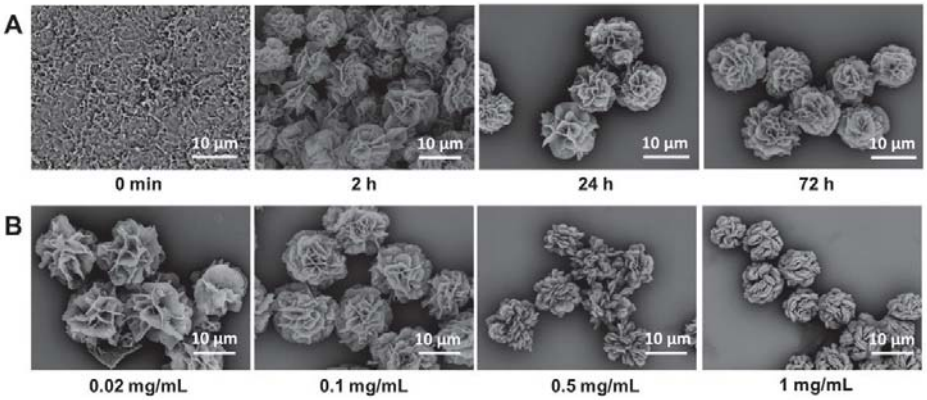

Figure 2. (A) Effect of different incubation times (0 min, 2 h, 24 h, 72 h) on the morphologies of the SA-$Cu_3(PO_4)_2$ HNFs. (B) The morphology of SA-$Cu_3(PO_4)_2$ HNFs prepared at various concentrations of SA (0.02, 0.1, 0.5 and 1 mg/mL).

In the preparation of the DNA-$Cu_3(PO_4)_2$ HNFs, SA was taken as a precursor. After adding SA and $CuSO_4$ into the PBS solution, Cu^{2+} could interact with amine groups from the SA and then the complexes were evolved into the primary crystals of copper phosphate, which in turn provided more nucleation sites for larger copper phosphate crystals (0 min, Figure. 2A). With the incubation time increased, more primary crystals combined into the large agglomerates and began to form the flower-like nanostructure (2h, 24h, Figure 2A). Finally, after incubation for 72 h (72h, Figure 2A), the flower-like nanostructure was completely formed. In this process, SA induced the formation of primary crystals for petals location and bound the petals together. The effect of SA concentrations was further investigated. As shown in Figure 2B, the morphology of the nanoflowers was dependent on the SA concentration. With the SA concentration increased from 0.02 to 1 mg/mL, the nucleation sites for petals formation were increased, leading to the formation of HNFs with smaller size, and more petals were agglomerated in one nanoflower with the decreased distances between the petals. In addition, the increased concentration of SA also resulted the increased DNA binding ability of these HNFs as verified by the fluorescence intensity (Figure S1), which indicated the percentage of the SA in the HNFs increased and more DNA could be bound to the nanoflowers.

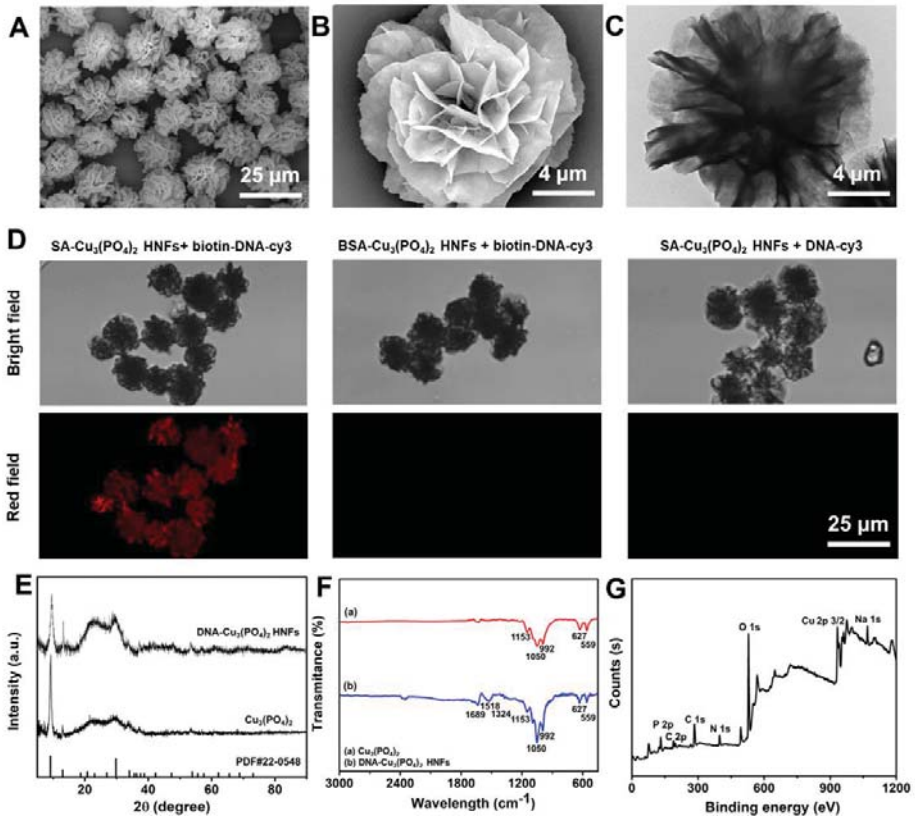

Figure 3. Characterization of DNA-$Cu_3(PO_4)_2$ HNFs. (A) and (B) SEM images of DNA-$Cu_3(PO_4)_2$ HNFs. (C) TEM images of DNA-$Cu_3(PO_4)_2$ HNFs. (D) Fluorescence microscope images of SA-$Cu_3(PO_4)_2$ HNFs with biotin-DNA-cy3, BSA-$Cu_3(PO_4)_2$ HNFs with biotin-DNA-cy3 and SA-$Cu_3(PO_4)_2$ HNFs with DNA-cy3. (E) XRD patterns of DNA-$Cu_3(PO_4)_2$ HNFs and $Cu_3(PO_4)_2$. (F) FT-IR spectra of $Cu_3(PO_4)_2$ and DNA-$Cu_3(PO_4)_2$ HNFs. (G) XPS pattern of DNA-$Cu_3(PO_4)_2$ HNFs.

The DNA-$Cu_3(PO_4)_2$ HNFs (synthesized by 0.1 mg/mL SA) were characterized systematically. SEM and TEM images were taken to investigate the morphology of the DNA-$Cu_3(PO_4)_2$ HNFs. It was observed that the hybrid products were assembled from numerous nanoplates and exhibited hierarchical peony-like nanostructure with good monodispersity and the size was 14 ± 1.5 μm (Figure 3A, B and C). The confocal laser

scanning microscope (CLSM) images visually displayed the successfully preparation of the DNA-$Cu_3(PO_4)_2$ HNFs (Figure 3D). Red fluorescence nanoflowers could be observed after the SA-$Cu_3(PO_4)_2$ HNFs incubated with biotin-DNA-cy3 (Figure 3D, left). But for BSA-$Cu_3(PO_4)_2$ HNFs, no red fluorescence could be observed after being incubated with the biotin-DNA-cy3 (Figure 3D, middle). Moreover, no fluorescence could be observed for SA-$Cu_3(PO_4)_2$ HNFs after incubation with the DNA-cy3 (Figure 3D, right). Based on the comparison, it can be deduced that the DNA-$Cu_3(PO_4)_2$ HNFs were formed by the specific interaction between SA and biotin. As shown in Figure 3E, the XRD analysis demonstrated that the inorganic component of the HNFs was $Cu_3(PO_4)_2$ according to the JCPDS card (PDF#22-0548). The FT-IR spectroscopy was also recorded (Figure 3F). The spectrum a and b both displayed the strong IR bands at 1050 cm^{-1} (the P-O vibrations and stretches) and the bands at 559 cm^{-1} and 627 cm^{-1} (the bending vibrations of bridging phosphorous), indicating the existence of phosphate groups in $Cu_3(PO_4)_2$ and DNA-$Cu_3(PO_4)_2$ HNFs. In comparison with spectrum a, the unique bands at 1400-1600 cm^{-1} could be observed in the IR spectrum of DNA-$Cu_3(PO_4)_2$ HNFs, which was ascribed to $–NH_2$ group in the protein and DNA, indicating the SA and DNA was successful immobilized to the DNA-$Cu_3(PO_4)_2$ HNFs. Furthermore, the XPS analysis of the DNA-$Cu_3(PO_4)_2$ HNFs (Figure 3G) convinced the existence of P, Cu, C, N and O elements, indicating the successful synthesis of the DNA-$Cu_3(PO_4)_2$ HNFs.

The migrating performance of DNA-$Cu_3(PO_4)_2$ HNFs on the cotton thread was studied. As shown in Figure S2, the DNA-$Cu_3(PO_4)_2$ HNFs could not migrate along the

cotton thread due to their large sizes and entrapped at the starting of the thread (Figure S2A). In comparison, free DNA could easily flow to the absorption pad (Figure S2B). Due to the different migrating performances between the DNA-$Cu_3(PO_4)_2$ HNFs and DNA, the DNA-$Cu_3(PO_4)_2$ HNFs can be taken as key captors to fabricate a facile thread platform for miRNA-21 detection.

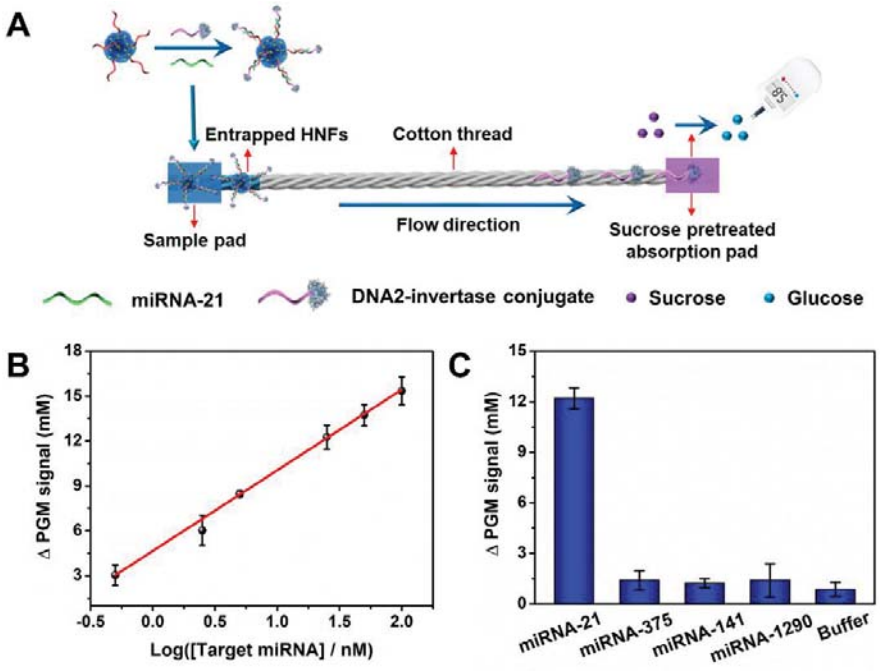

Figure 4. (A) Schematic illustration of the measurement principle of the miRNA biosensor. (B) The resulting calibration curve of the △ PGM signal of the cotton thread-based biosensor versus target miRNA-21 logarithm concentration. (C) Selectivity of the cotton thread-based biosensor. The △ PGM signal in the presence of 25 nM of miRNA-21, miRNA-375, miRNA-141, miRNA-1290 and buffer solution.

Principle of the miRNA biosensor. Due to the excellent characteristics of the DNA-$Cu_3(PO_4)_2$ HNFs including high stability, large surface-to-volume ratio, high DNA

encapsulation ability and large size induced low migration mentioned above, the HNFs can be exploited to fabricate a facile miRNA biosensor combining cotton thread as the microfluidic channel and PGM as signal readout. The principle of miRNA detection based on bioinspired DNA-inorganic HNFs are illustrated in Figure 4A. With the existence of miRNA-21, a sandwich structure of "HNF-DNA1 / miRNA / DNA2-invertase" is formed and the free DNA2-invertase conjugates are captured to the HNFs. Then the mixtures are applied to the sample pad, the HNFs will be entrapped at the starting of the cotton thread due to the large size while the surplus free DNA2-invertase conjugates will migrate towards to the sucrose pad through the capillary action. The sucrose which is firstly immobilized on the absorption pad can be catalyzed into glucose by DNA2-invertase conjugates and the glucose concentration can be quantified by a PGM. The change of PGM signal before and after the miRNA detection is used to evaluate the miRNA-21 concentration.

Optimization of assay conditions. The assay conditions including the reaction time, the concentration of SA used to prepare the SA-$Cu_3(PO_4)_2$ HNFs, DNA1 bound to the SA-$Cu_3(PO_4)_2$ HNFs, the amount of the DNA2-invertase conjugates and the amount of the DNA-$Cu_3(PO_4)_2$ HNFs were discussed in this study and optimized through a series of experiments.

The reaction time for invertase catalysis is very important for the performance of the biosensor. 1 μL DNA2-invertase conjugates solution was added into the sample pad, and the glucose concentration of the absorption pad was monitored by a PGM at

different time points. Figure S3 displayed that the PGM signal reached maximum at 70 min and kept at a steady value in the following time. Thus 70 min was the optimized reaction time.

The concentration of the SA used to prepare the SA-$Cu_3(PO_4)_2$ HNFs is corrected with DNA encapsulation ability of nanoflowers and then further influence the miRNA detection. Four different concentrations of SA (0.02, 0.1, 0.5, 1 mg/mL) were used to prepare nanoflowers. As demonstrated in Figure S4, all the four kinds of HNFs could be entrapped at the starting of the thread after applying them to the cotton thread-based device and could be applied to fabricate the miRNA biosensors. As demonstrated in Figure S5A, the largest △ PGM signal was obtained at the concentration of 0.1 mg/mL and kept steady with the further rise of the concentration of SA, indicating the amount of DNA labelled on the HNFs prepared at 0.1mg/mL SA was sufficient for miRNA-21 detection. Thus the concentration of SA used for SA-$Cu_3(PO_4)_2$ HNFs preparation in the following study was 0.1 mg/mL.

The amount of DNA1 on the SA-$Cu_3(PO_4)_2$ HNFs is significant for DNA1 and miRNA-21 hybridization, and further influence the sensitivity of the biosensor. As demonstrated in Figure S5B, with the increase of DNA1, the △ PGM signal increased and kept stable after the concentration reached 7 μM. So the optimal concentration of the DNA1 was 7 μM and was used in the following experiments.

The amount of DNA2-invertase conjugates also influence the sensitivity of the miRNA biosensor. To this regard, we studied the effect of the DNA2-invertase

conjugates by adding different volumes, it can be seen that △ PGM signal was increased at first amount from 0.2 to 0.8 μL and then reached saturation (Figure S5C). Therefore, 0.8 μL of DNA2-invertase conjugates were applied in the following study.

The performance of the cotton thread-based biosensor is also relevant to the amount of the DNA-$Cu_3(PO_4)_2$ HNFs. More DNA-$Cu_3(PO_4)_2$ HNFs can hybridize with more target miRNA-21 and thus can capture more DNA2-invertase conjugates into the HNFs. As shown in Figure S5D, with the increase of the volume of DNA-$Cu_3(PO_4)_2$ HNFs to 5 μL, the △ PGM signal increased to maximum. Thus 5 μL was the optimal amount of the DNA-$Cu_3(PO_4)_2$ HNFs and used in the following study.

Analytical characteristics. The analytical performance of the cotton thread-based biosensor was evaluated by measuring miRNA-21 in different concentrations ranging from 0.5 to 100 nM under the optimized experimental conditions. The △ PGM signal was increased with the increase of the concentration of miRNA-21 and exhibited a good linear relationship with the logarithm concentration of miRNA-21 (Figure 4B). The limit of the detection of the cotton thread based biosensor was 0.41 nM (based on S/N=3).

Then the selectivity was further investigated. Three interference miRNAs including miRNA-375, miRNA-141 and miRNA-1290 at the concentration of 25 nM were applied to this miRNA biosensor to assess the selectivity. As demonstrated in Figure 4C, the interference miRNAs displayed no distinct response and the △ PGM signal was almost the same as the background. However, the △ PGM signal was high

of the target miRNA-21, which is beneficial from the specific hybridization between DNA1, target miRNA21 and DNA2, indicating high selectivity of this cotton thread-based biosensor.

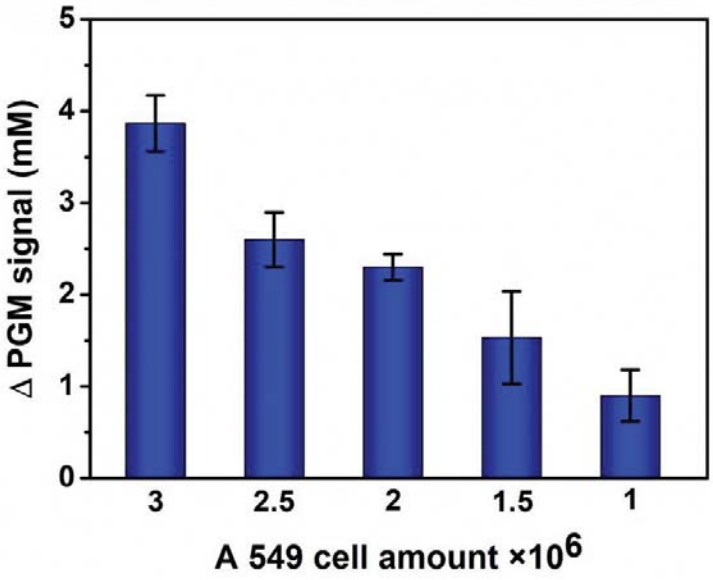

Figure 5. Detection of miRNA-21 in cell lysate. The △ PGM signal with the existence of different amounts of A549 cells: 3, 2.5, 2, 1.5 and 1 million.

Analysis of miRNA-21 in A549 cell lysate. The results mentioned above showed the proposed miRNA biosensor owned good sensitivity and high selectivity, which triggered us to assess the capability of this biosensor in biological sample. The cotton thread-based biosensor was applied for miRNA-21 detection in A549 cell lysate. Typically, 10 μL of A549 cell lysate containing various amounts of A549 cells were added to 40 μL PBS solution and then tested by the miRNA biosensors. Figure 5 showed the results, with the decrease of the lysed A549 cells, the △ PGM signal decreased, and the miRNA-21 in as low as one million A549 cell lysates could be

detected. Thus the proposed biosensor exhibited high specificity and strong anti-interference ability and held great potential in clinical application.

CONCLUSIONS

In summary, the bioinspired DNA-$Cu_3(PO_4)_2$ HNFs were successfully synthesized and the resultant nanoflowers showed sophisticate structures, high stability, large surface-to-volume ratio, high DNA encapsulation and miRNA recognition ability. Based on the bioinspired DNA-$Cu_3(PO_4)_2$ HNFs as the key captors, a facile thread platform for miRNA detection has been fabricated by using cotton thread as the microfluidic channel and PGM as signal readout. In the presence of miRNA, the HNFs could capture the DNA-invertase conjugates and be entrapped at the starting of a cotton thread while the surplus DNA-invertase conjugates could be transported to the absorption pad where the invertase in conjugates hydrolyzed the sucrose into glucose, and then a PGM was used to quantify the glucose concentration. The proposed strategies for miRNA-21 detection showed good sensitivity and selectivity, a detection limit of 0.41 nM was achieved under the optimal conditions. Furthermore, the proposed biosensor displayed good anti-interference ability of other components in the real biological sample, the miRNA-21 in A549 cell lysate could be easily detected without complex purification or separation producers. Such attractive miRNA biosensor based on bioinspired DNA-$Cu_3(PO_4)_2$ HNFs, cotton thread and PGM shows good sensitivity, selectivity and anti-interference performance, which offers an alternative tool for

quantitative detection of miRNA in POC settings and shows great promise in biomedical and clinical applications.

ASSOCIATED CONTENT

Supporting Information.

The Supporting Information is available free of charge on the ACS Publications website.

Additional information as noted in the text, including the fluorescence spectra, the migrating performance of the DNA-$Cu_3(PO_4)_2$ HNFs, optimization of assay conditions and the electrophoresis images.

AUTHOR INFORMATION

Corresponding Author

***E-mail:** xuliping@ustb.edu.cn

***E-mail:** zhangxueji@ustb.edu.cn

Notes

The authors declare no competing financial interest.

ACKNOWLEDGEMENTS

The work is supported by National Natural Science Foundation of China (NSFC Grant no. 21475008, 21475009), Beijing Municipal Science & Technology Commission (Z161100000116037) and Beijing Natural Science Foundation (Grant No. 2182036).

REFERENCES

(1) Wang, Z.; Huang, P.; Jacobson, O.; Wang, Z.; Liu, Y.; Lin, L.; Lin, J.; Lu, N.; Zhang, H.; Tian, R.; Niu, G.; Liu, G.; Chen, X. Biomineralization-Inspired Synthesis of Copper Sulfide-Ferritin Nanocages as Cancer Theranostics. *ACS Nano* **2016,** *10* (3), 3453-3601.

(2) Yao, S.; Jin, B.; Liu, Z.; Shao, C.; Zhao, R.; Wang, X.; Tang, R. Biomineralization: From Material Tactics to Biological Strategy. *Adv. Mater.* **2017,** *29* (14), 1605903.

(3) Nudelman, F.; Sommerdijk, N. A. Biomineralization as an inspiration for materials chemistry. *Angew. Chem. Int. Ed.* **2012,** *51* (27), 6582-6596.

(4) Jin, W.; Jiang, S.; Pan, H.; Tang, R. Amorphous Phase Mediated Crystallization: Fundamentals of Biomineralization. *Crystals* **2018,** *8* (1), 48.

(5) Li, W.; Lu, S.; Bao, S.; Shi, Z.; Lu, Z.; Li, C.; Yu, L. Efficient in situ growth of enzyme-inorganic hybrids on paper strips for the visual detection of glucose. *Biosens. Bioelectron.* **2018,** *99*, 603-611.

(6) Liu, Y.; Chen, J.; Du, M.; Wang, X.; Ji, X.; He, Z. The preparation of dual-functional hybrid nanoflower and its application in the ultrasensitive detection of disease-related biomarker. *Biosens. Bioelectron.* **2017,** *92*, 68-73.

(7) Ge, J.; Lei, J.; Zare, R. N. Protein–inorganic hybrid nanoflowers. *Nat. Nanotechnol.* **2012,** *7* (7), 428-432.

(8) Ye, R.; Zhu, C.; Song, Y.; Lu, Q.; Ge, X.; Yang, X.; Zhu, M.-J.; Du, D.; Li, H.; Lin, Y. Bioinspired Synthesis of All-in-One Organic-Inorganic Hybrid Nanoflowers

Combined with a Handheld pH Meter for On-Site Detection of Food Pathogen. *Small* **2016,** *12* (23), 3094-3100.

(9) Lin, Z.; Xiao, Y.; Yin, Y.; Hu, W.; Liu, W.; Yang, H. Facile Synthesis of Enzyme-Inorganic Hybrid Nanoflowers and Its Application as a Colorimetric Platform for Visual Detection of Hydrogen Peroxide and Phenol. *ACS Appl. Mater. Interfaces* **2014,** *6* (13), 10775-10782.

(10) Huang, Y.; Ran, X.; Lin, Y.; Ren, J.; Qu, X. Self-assembly of an organic–inorganic hybrid nanoflower as an efficient biomimetic catalyst for self-activated tandem reactions. *Chem. Commun.* **2015,** *51* (21), 4386-4389.

(11) Yin, Y.; Xiao, Y.; Lin, G.; Xiao, Q.; Lin, Z.; Cai, Z. An enzyme–inorganic hybrid nanoflower based immobilized enzyme reactor with enhanced enzymatic activity. *J. Mater. Chem. B* **2015,** *3* (11), 2295-2300.

(12) Sun, J.; Ge, J.; Liu, W.; Lan, M.; Zhang, H.; Wang, P.; Wang, Y.; Niu, Z. Multi-enzyme co-embedded organic–inorganic hybrid nanoflowers: synthesis and application as a colorimetric sensor. *Nanoscale* **2014,** *6* (1), 255-262.

(13) Hu, R.; Zhang, X.; Zhao, Z.; Zhu, G.; Chen, T.; Fu, T.; Tan, W. DNA nanoflowers for multiplexed cellular imaging and traceable targeted drug delivery. *Angew. Chem. Int. Ed.* **2014**, *53* (23), 5821-5826.

(14) Meng, H. M.; Liu, H.; Kuai, H.; Peng, R.; Mo, L.; Zhang, X. B. Aptamer-integrated DNA nanostructures for biosensing, bioimaging and cancer therapy. *Chem. Soc. Rev.* **2016**, *45* (9), 2583-2602.

(15) Zhu, G.; Hu, R.; Zhao, Z.; Chen, Z.; Zhang, X.; Tan, W. Noncanonical self-assembly of multifunctional DNA nanoflowers for biomedical applications. *J. Am. Chem. Soc.* **2013,** *135* (44), 16438-16445.

(16) Ge, Z.; Lin, M.; Wang, P.; Pei, H.; Yan, J.; Shi, J.; Huang, Q.; He, D.; Fan, C.; Zuo, X. Hybridization chain reaction amplification of microRNA detection with a tetrahedral DNA nanostructure-based electrochemical biosensor. *Anal. Chem.* **2014,** *86* (4), 2124-2130.

(17) Zhou, H.; Yang, C.; Chen, H.; Li, X.; Li, Y.; Fan, X. A simple G-quadruplex molecular beacon-based biosensor for highly selective detection of microRNA. *Biosens. Bioelectron.* **2017,** *87*, 552-557.

(18) Ventura, A.; Jacks, T. MicroRNAs and cancer: short RNAs go a long way. *Cell* **2009,** *136* (4), 586-91.

(19) Dong, H.; Lei, J.; Ding, L.; Wen, Y.; Ju, H.; Zhang, X. MicroRNA: function, detection, and bioanalysis. *Chem. Rev.* **2013,** *113* (8), 6207-6233.

(20) Chen, D.; Taylor, K. P.; Hall, Q.; Kaplan, J. M. The Neuropeptides FLP-2 and PDF-1 Act in Concert To Arouse Caenorhabditis elegans Locomotion. *Genetics* **2016,** *204* (3), 1151-1159.

(21) Jia, H.; Li, Z.; Liu, C.; Cheng, Y. Ultrasensitive detection of microRNAs by exponential isothermal amplification. *Angew. Chem. Int. Ed.* **2010,** *49* (32), 5498-5501.

(22) Peng, Y.; Zhou, W.; Yuan, R.; Xiang, Y. Dual-input molecular logic circuits for sensitive and simultaneous sensing of multiple microRNAs from tumor cells. *Sens. Actuator B Chem.* **2018,** *264*, 202-207.

(23) Zheng, W.; Yao, L.; Teng, J.; Yan, C.; Qin, P.; Liu, G.; Chen, W. Lateral flow test for visual detection of multiple MicroRNAs. *Sens. Actuator B Chem.* **2018,** *264*, 320-326.

(24) Lu, L. M.; Zhang, X. B.; Kong, R. M.; Yang, B.; Tan, W. A ligation-triggered DNAzyme cascade for amplified fluorescence detection of biological small molecules with zero-background signal. *J. Am. Chem. Soc.* **2011**, *133* (30), 11686-11691.

(25) Gao, X.; Xu, L. P.; Wu, T.; Wen, Y.; Ma, X.; Zhang, X. An enzyme-amplified lateral flow strip biosensor for visual detection of microRNA-224. *Talanta* **2016,** *146*, 648-654.

(26) Gao, X.; Xu, H.; Baloda, M.; Gurung, A. S.; Xu, L. P.; Wang, T.; Zhang, X.; Liu, G. Visual detection of microRNA with lateral flow nucleic acid biosensor. *Biosens. Bioelectron.* **2014,** *54*, 578-584.

(27) Wu, T.; Xu, T.; Xu, L. P.; Huang, Y.; Shi, W.; Wen, Y.; Zhang, X. Superhydrophilic cotton thread with temperature-dependent pattern for sensitive nucleic acid detection. *Biosens. Bioelectron.* **2016,** *86*, 951-957.

(28) Lin, B.; Liu, D.; Yan, J.; Qiao, Z.; Zhong, Y.; Yan, J.; Zhu, Z.; Ji, T.; Yang, C. J. Enzyme-Encapsulated Liposome-Linked Immunosorbent Assay Enabling Sensitive Personal Glucose Meter Readout for Portable Detection of Disease Biomarkers. *ACS Appl. Mater. Interfaces* **2016,** *8* (11), 6890-6897.

(29) Lan, T.; Zhang, J.; Lu, Y. Transforming the blood glucose meter into a general healthcare meter for in vitro diagnostics in mobile health. *Biotechnol. Adv.* **2016,** *34* (3), 331-341.

(30) Gao, Z.; Tang, D.; Xu, M.; Chen, G.; Yang, H. Nanoparticle-based pseudo hapten for target-responsive cargo release from a magnetic mesoporous silica nanocontainer. *Chem. Commun.* **2014,** *50* (47), 6256-6258.

(31) Zhang, J.; Shen, Z.; Xiang, Y.; Lu, Y. Integration of Solution-Based Assays onto Lateral Flow Device for One-Step Quantitative Point-of-Care Diagnostics Using Personal Glucose Meter. *ACS Sensors* **2016,** *1* (9), 1091-1096.

(32) Fang, D.; Gao, G.; Yu, Y.; Shen, J.; Zhi, J. Adaptive use of a personal glucose meter (PGM) for acute biotoxicity assessment based on the glucose consumption of microbes. *Analyst* **2016,** *141* (10), 3004-3011.

(33) Yan, L.; Zhu, Z.; Zou, Y.; Huang, Y.; Liu, D.; Jia, S.; Xu, D.; Wu, M.; Zhou, Y.; Zhou, S.; Yang, C. J. Target-responsive "sweet" hydrogel with glucometer readout for portable and quantitative detection of non-glucose targets. *J. Am. Chem. Soc.* **2013,** *135* (10), 3748-3751.

(34) Xiang, Y.; Lu, Y. Using personal glucose meters and functional DNA sensors to quantify a variety of analytical targets. *Nat. Chem.* **2011,** *3* (9), 697-703.

(35) Huang, H.; Zhao, G.; Dou, W. Portable and quantitative point-of-care monitoring of Escherichia coli O157:H7 using a personal glucose meter based on immunochromatographic assay. *Biosens. Bioelectron.* **2018,** *107*, 266-271.

(36) Gu, C.; Lan, T.; Shi, H.; Lu, Y. Portable Detection of Melamine in Milk Using a Personal Glucose Meter Based on an in Vitro Selected Structure-Switching Aptamer. *Anal. Chem.* **2015,** *87* (15), 7676-7682.

(37) Zhou, Z.; Xiang, Y.; Tong, A.; Lu, Y. Simple and efficient method to purify DNA-protein conjugates and its sensing applications. *Anal. Chem.* **2014,** *86* (8), 3869-3875.

TOC graphic